Collective properties of the odd-mass I nuclei: ^{117,119,121}I

M. Gai,* D. M. Gordon,† R. E. Shroy,‡ and D. B. Fossan
Department of Physics, State University of New York, Stony Brook, New York 11794

A. K. Gaigalas§
Department of Physics, State University of New York, Binghamton, New York 13901

(Received 7 April 1982)

The high-spin states of ^{117,119,121}I have been investigated by in-beam γ-ray spectroscopy via the ^{A}Sn(^{6}Li,3n)$^{A+3}$I reactions to study the collective properties of the odd-mass I isotopes. A similar study of ^{123,125,127}I is reported in the preceding paper. Two collective features have been observed: $\Delta J=1$ bands built on low-lying $\frac{9}{2}^+$ proton-hole states and $\Delta J=2$ bands built on $\frac{11}{2}^-$, $\frac{7}{2}^+$, and $\frac{5}{2}^+$ quasiproton states. The $\Delta J=2$ energy spacings for the $\frac{11}{2}^-$ bands decrease significantly relative to those for the ground-state bands of the Te core nuclei as A decreases, but not for the $\frac{7}{2}^+$ and $\frac{5}{2}^+$ $\Delta J=2$ bands. This unexpected decrease can be explained in a generalized seniority scheme. The systematic properties of the $\Delta J=2$ bands for all of the odd-mass I isotopes are summarized. These collective properties are examined in terms of both the microscopic and phenomenological approaches. Pulsed-beam-γ measurements yielded mean lifetimes of $\tau=17.5\pm1.0$, 41.5 ± 1.5, and 13.5 ± 0.5 ns for the $\frac{9}{2}^+$ proton-hole states in ^{117,119,121}I, respectively. These values imply hindrances of $\sim10^4$ relative to $M1$ Weisskopf estimates for the transitions to the $\frac{7}{2}^+$ quasiproton states. A spin rotation measurement yielded a g factor for the $\frac{9}{2}^+$ isomer in ^{119}I of $g=1.21\pm0.08$. Another isomer with a mean life of $\tau=13\pm2$ μs was observed at 2377 keV in ^{121}I.

NUCLEAR REACTIONS $^{114-118}$Sn(^{6}Li,3n)$^{117-121}$I; measured γ-γ-t coincidences, $\gamma(E, \theta, t)$, spin rotation in $B=13.4$ kG; deduced level schemes in odd-mass $^{117-121}$I, γ multipolarities, J^π, $T_{1/2}$, g factor. Enriched targets, Ge(Li) detectors.

I. INTRODUCTION

The experimental investigations of high-spin states in the odd-proton nuclei of the $Z\gtrsim50$ transition region have revealed two collective features that have been systematically observed as a function of neutron number for the Sb ($Z=51$) (Refs. 1–3), I ($Z=53$) (Refs. 3–5), Cs ($Z=55$) (Refs. 6 and 7), and La ($Z=57$) (Refs. 3 and 8) nuclei. One collective feature involves $\Delta J=2$ bands built on the $\frac{11}{2}^-$, $\frac{7}{2}^+$, and $\frac{5}{2}^+$ quasiproton states. The $\Delta J=2$ band spacings generally follow the spacings of the ground-state bands of the corresponding even core nuclei with the exception of the $\frac{11}{2}^-$ bands in the odd-mass I nuclei,[4] where the spacings decrease significantly relative to those of the Te cores as A decreases. The other collective feature of this transition region is the $\Delta J=1$ bands built on the low-lying $\frac{9}{2}^+$ proton-hole states. The $\frac{9}{2}^+$ bandheads were observed to drop to very low energy in the middle of the neutron shell.

The complete experimental results of the odd-mass I nuclei which were obtained from γ-ray studies following (^{6}Li,3n) fusion-evaporation reactions are presented in the preceding paper (I) and the present paper (II). Paper I covers the results for ^{123,125,127}I and summarizes the $\Delta J=1$ band systematics. The experimental results for ^{117,119,121}I are given in paper II along with a summary and discussion of the systematics of the $\Delta J=2$ bands in all of the odd-mass I nuclei. The surprising result obtained from the systematics, that the $\Delta J=2$ energy

spacings for the $1h_{11/2}$ quasiproton states in the odd-mass I isotopes decrease relative to those for the Te cores as A decreases, can be explained microscopically[9] in terms of a generalized seniority scheme involving the number of core neutrons in an effective shell. Theoretical considerations in terms of both microscopic and phenomenological approaches for these collective properties will be examined.

Very little previous experimental information was available on ^{117,119,121}I.[10] During the course of this study, some high-spin experimental information on ^{121}I has become available from a ^{121}Sb(^{3}He,3n)^{121}I study.[11] An experiment[3] involving the ^{106}Cd(^{17}N,2pn)^{117}I reaction confirmed the present results for ^{117}I and yielded additional high-spin information. Recently, experimental information on high-spin states in ^{115}I has been obtained in this laboratory via the ^{106}Cd(^{12}C,$p2n$)^{115}I reaction,[3] which extends the collective systematics to the next lower mass.

II. EXPERIMENTAL PROCEDURE

The high-spin level structures of the odd-mass ^{117,119,121}I nuclei were studied by in-beam γ-ray measurements following (^{6}Li,3n) fusion-evaporation reactions. Self-supporting enriched metal foils of ^{114,116,118}Sn were used as targets. The enrichment of the ^{114}Sn target was 64% which added background for the ^{114}Sn(^{6}Li,3n)^{117}I study. The enrichment of all the other Sn targets in this study were $>92\%$. The following set of γ-ray measurements were performed on these targets: γ excitation, γ-γ coincidences, γ-angular distributions, and pulsed beam-γ timing measurements. The details of the experimental procedures have been described in paper I. In addition to delayed γ-ray spectra, time-differential pulsed beam-γ experiments were made to measure lifetimes for the isomers located in ^{117,119,121}I. A time differential perturbed angular distribution (TDPAD) g-factor measurement was also made for the $\frac{9}{2}^{+}$ isomer in ^{119}I. The details of this TDPAD measurement will be given with the ^{119}I results in the next section.

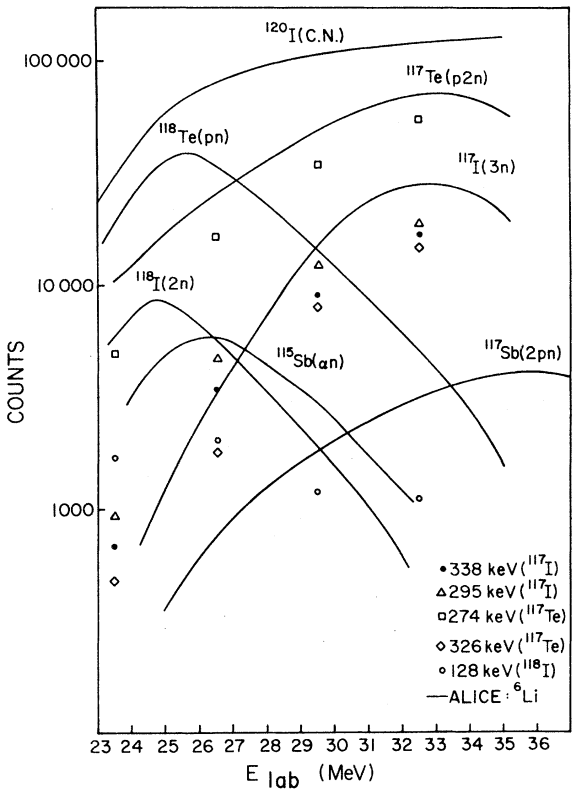

FIG. 1. The ^{6}Li + ^{114}Sn excitation functions observed for ground-state γ rays of several residual nuclei. Comparison ALICE calculations for the various channels are shown by the solid curves. These results show the competing reactions in the study of the neutron deficient ^{117}I nucleus via the (^{6}Li,3n) reaction.

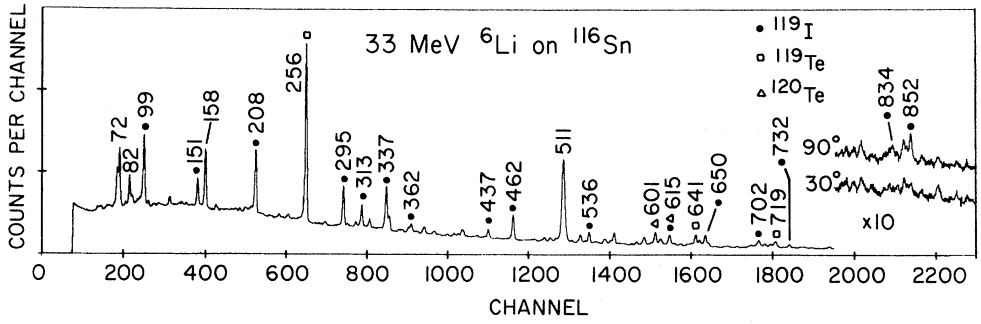

FIG. 2. γ-ray singles spectrum observed with a Ge(Li) detector for the bombardment of a ^{116}Sn target with a 33-MeV ^{6}Li beam.

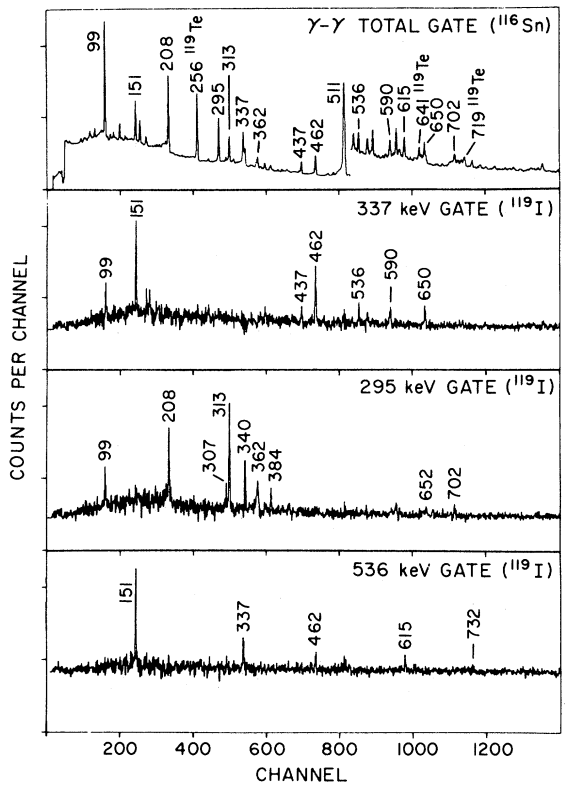

FIG. 3. Representative γ-γ coincidence spectra from the ^{116}Sn(^{6}Li,3n)^{119}I reaction for selected γ-ray gates.

III. EXPERIMENTAL RESULTS

The γ-ray excitation results for the ^{114,116,118}Sn targets showed that the (^{6}Li,p 2n) channel populating the odd-mass Te nuclei becomes increasingly important compared to the (^{6}Li,3n) channel for the lower mass Sn targets. This results from the rapid decrease in the proton binding energy as the neutron number decreases from the line of stability. Thus, the studies of the neutron deficient ^{117}I nucleus and to a lesser extent ^{119}I are made difficult because of background from the (^{6}Li,p 2n) channel. The ^{6}Li+^{114}Sn excitation functions of ground-state γ rays for the various residual nuclei are compared with an ALICE[12] calculation in Fig. 1; they show the competing channels for the ^{117}I study. The singles γ-ray spectrum for 33 MeV ^{6}Li on the ^{116}Sn target displayed in Fig. 2 identifies the γ-ray competition for the ^{119}I study.

Because of both the reaction and target difficulties for the ^{117}I study, additional reactions were examined to aid in the determination of the ^{117}I γ-ray transitions. Singles γ-ray spectra were measured for 42 MeV ^{10}B on an enriched ^{110}Cd target to observe the ^{110}Cd(^{10}B,3n)^{117}I and ^{110}Cd(^{10}B,p2n)^{117}Te reaction channels and for 18 MeV α particles on ^{114}Sn to observe the ^{114}Sn(α,n)^{117}Te channel. A subsequent γ-ray study[3] via ^{106}Cd(^{14}N,2pn)^{117}I confirmed the results for ^{117}I from the present experiment as well as adding information for higher spin states because of the increased angular momentum. For the ^{119}I study, an examination of the ^{116}Sn(α,n)^{119}Te reaction was also made.

The γ-γ coincidence information was obtained via the (^{6}Li,3n) reaction. Typical γ-γ coincidence spectra are shown in Fig. 3 for ^{119}I. The angular distribution information obtained for ^{117,119,121}I is given in Tables I–III, respectively. The high-spin level structures and γ-ray decay schemes of ^{117,119,121}I deduced from these γ-ray results are shown, respectively, in Figs. 4–6.

The two common collective features observed in ^{123,125,127}I also appeared systematically in the ^{117,119,121}I nuclei. The first is $\Delta J=2$ γ-ray cascades built on low-lying $\frac{11}{2}^-$, $\frac{7}{2}^+$, and $\frac{5}{2}^+$ levels. The angular distributions of the cascade members yielded A_2 and A_4 coefficients characteristic of pure $J\rightarrow J-2$ quadrupole transitions. The spacings in these $\Delta J=2$ cascades are fairly similar to the spacings of the corresponding even-mass Te core nuclei with the exception of the lower-mass I $\frac{11}{2}^-$ bands, where the spacings decrease continually as A decreases reaching a factor of $\frac{1}{2}$ relative to the spacings of the Te cores.

The second collective feature common to these odd-mass I nuclei is a series of $\Delta J=1$ cascades built on low-lying $\frac{9}{2}^+$ states. The angular distributions of the γ rays belonging to these cascades exhibit a mixed $M1$-$E2$ character with a positive mixing ratio δ. The $M1$-$E2$ character of the $\Delta J=1$ cascades is further corroborated by the observation of $J\rightarrow J-2$ $E2$ crossover transitions.

In addition to these band structures, the $\frac{9}{2}^+$ states, that are fed by the low-lying $\frac{11}{2}^-$ states but are not band members in the ^{123,125,127}I nuclei, were also observed at 650 keV in the ^{119,121}I nuclei. In ^{117}I, the 620 keV $\frac{9}{2}^+$ state is possibly the first member of the $\frac{5}{2}^+$ $\Delta J=2$ band from systematics. For ^{121}I, as also observed in ^{123}I, a second low-lying $\frac{7}{2}^+$ state ($\sim$450 keV) was observed to be fed by a $\Delta J=2$ cascade of γ rays. The $\frac{5}{2}^+$ ground-state J^π assignment is known[10] in ^{121}I; this assignment, which is assumed for ^{117,119}I, is consistent with the observed systematics. The information obtained for ^{121}I from the independent (^{3}He,3n) study[11] is in agreement with the present results where overlap occurs.

TABLE I. Angular distribution results for ^{117}I.

E_γ (keV)[a]	I_γ[b]	A_2	A_4	Branching ratio (B.R.) (%)[c]	$J_i^\pi \rightarrow J_f^\pi$	$\delta(E2/M1)$[d]
58.4		−0.03±0.15			$\frac{7}{2}^+ \rightarrow \frac{5}{2}^+$	
294.8	100	−0.11±0.06	−0.20±0.20	93±2	$\frac{9}{2}^+ \rightarrow \frac{7}{2}^+$	0.05±0.05
300.6	60	−0.02±0.07	−0.20±0.20		$\frac{11}{2}^+ \rightarrow \frac{9}{2}^+$	0.14±0.05
317.9	35	−0.07±0.09	−0.20±0.20		$\frac{13}{2}^+ \rightarrow \frac{11}{2}^+$	0.10±0.05
337.5	66	0.30±0.08	−0.09±0.08		$\frac{15}{2}^- \rightarrow \frac{11}{2}^-$	
346.3	17	−0.02±0.10	−0.05±0.20		$\frac{15}{2}^+ \rightarrow \frac{13}{2}^+$	0.14±0.05
353.4	8			7±2	$\frac{9}{2}^+ \rightarrow \frac{5}{2}^+$	
368±1						
470.8	38	0.29±0.13	−0.18±0.10		$\frac{19}{2}^- \rightarrow \frac{15}{2}^-$	
605±1[e]	32				$\frac{11}{2}^- \rightarrow \frac{7}{2}^+$	
619.7	36				$\frac{9}{2}^+ \rightarrow \frac{5}{2}^+$	
663.1	42				$\frac{11}{2}^- \rightarrow \frac{5}{2}^+$	
714±1						

[a]Energies are accurate to within ±0.3 keV unless otherwise noted.
[b]I_γ, the relative intensities, have been normalized to a strong low-lying transition; typical uncertainties are ±10% except where noted.
[c]B.R. are the branching ratios of transitions from a given initial state.
[d]The $\delta(E2/M1)$ mixing ratios were extracted from the angular distribution results following Ref. 23 (paper I). An average value of the m-substate population half-width $\sigma=2.2\pm0.3$, which was obtained from pure multipolarities for the (^{6}Li,3n) reaction in this region, was assumed.
[e]Doublet unresolved in the singles spectrum; evidence from coincidence data.

Specific details appropriate to the individual level schemes of the ^{117,119,121}I nuclei will be discussed separately below. This includes the pulsed beam-γ lifetime measurements and the TDPAD g-factor experiment carried out for the observed isomers.

A. ^{117}I

The pulsed beam-γ measurements, which were described in paper I, revealed the 295- and 353-keV γ rays in ^{117}I to be delayed. The time differential spectra for the Compton subtracted photopeaks of both of these γ rays yielded the same lifetime from single lifetime fits. The time spectrum and fit for the 295-keV $\frac{9}{2}^+ \rightarrow \frac{7}{2}^+$ transition are shown in the lower left part of Fig. 7; an appropriate prompt resolution function is shown on the right. Since the time spectrum for both γ rays showed no prompt component, the ^{117}I isomer is identified as the 353-keV $\frac{9}{2}^+$ state. The mean lifetime obtained is $\tau=17.5\pm1.0$ ns.

B. ^{119}I

The 208- and 307-keV γ-ray transitions, that represent the decay of the 307-keV $\frac{9}{2}^+$ level in ^{119}I, were observed to be delayed in the pulsed beam-γ measurements. The time differential spectra for the Compton subtracted photopeaks of both of these γ rays yielded the same lifetime with no prompt components. Fits of these time spectra resulted in a mean lifetime $\tau=41.5\pm1.5$ ns for the 307-keV $\frac{9}{2}^+$ state in ^{119}I. The time spectrum and fit for the 208-keV decay transition are shown in the upper left part of Fig. 7.

A measurement of the g factor for this 307-keV isomer was carried out via the time-differential perturbed angular distribution (TDPAD) technique.[13] The pulsed beam-γ time spectra, I (135°,t) and I (−135°,t), for the TDPAD experiment were accumulated using the photopeaks of the 208-keV γ ray from two Ge(Li) detectors. An external field of $B=13.4$ kG perpendicular to the beam direction was used. To reduce possible alignment losses due

TABLE II. Angular distribution results for ^{119}I.

E_γ (keV)[a]	I_γ[b]	A_2	A_4	Branching ratio (B.R.) (%)[c]	$J_i^\pi \rightarrow J_f^\pi$	$\delta(E2/M1)$[d]
99.0		−0.08±0.08			$\frac{7}{2}^+ \rightarrow \frac{5}{2}^+$	0.06±0.09
151.0	28	−0.12±0.06			$\frac{11}{2}^- \rightarrow \frac{9}{2}^+$	
207.9	100	−0.05±0.06	−0.11±0.09	93±2	$\frac{9}{2}^+ \rightarrow \frac{7}{2}^+$	0.10±0.05
294.7	71	−0.01±0.08	−0.01±0.10		$\frac{11}{2}^+ \rightarrow \frac{9}{2}^+$	0.15±0.05
307.3	8			7±2	$\frac{9}{2}^+ \rightarrow \frac{5}{2}^+$	
312.6	49	0.04±0.06	−0.16±0.08		$\frac{13}{2}^+ \rightarrow \frac{11}{2}^+$	0.18±0.05
336.8	100	0.25±0.06	−0.20±0.08		$\frac{15}{2}^- \rightarrow \frac{11}{2}^-$	
339.7	31	−0.01±0.07	−0.03±0.09	74±4	$\frac{15}{2}^+ \rightarrow \frac{13}{2}^+$	0.15±0.05
361.8	26	−0.01±0.09	−0.11±0.12		$\frac{17}{2}^+ \rightarrow \frac{15}{2}^+$	0.15±0.05
384.1	9	−0.05±0.12	−0.05±0.16		$\frac{19}{2}^+ \rightarrow \frac{17}{2}^+$	0.13±0.05
437.2	40	−0.33±0.06	−0.13±0.09	50±5	$\frac{9}{2}^+ \rightarrow \frac{7}{2}^+$	−0.18±0.11
461.7	93	0.10±0.06	−0.20±0.08		$\frac{19}{2}^- \rightarrow \frac{15}{2}^-$	
536.1	41	0.39±0.08	−0.07±0.10	50±5	$\frac{9}{2}^+ \rightarrow \frac{5}{2}^+$	
550.8	27	−0.78±0.20		30±4	$\frac{9}{2}^+ \rightarrow \frac{7}{2}^+$	$-0.50 < \delta < 1.5$
590.1	34	0.36±0.10	−0.19±0.13		$\frac{23}{2}^- \rightarrow \frac{19}{2}^-$	
606.5[e]	<31	0.31±0.09			$\frac{13}{2}^+ \rightarrow \frac{9}{2}^+$	
615.1[e]	51	0.26±0.08			$\frac{13}{2}^+ \rightarrow \frac{9}{2}^+$	
652.6	11	0.28±0.20		26±4	$\frac{15}{2}^+ \rightarrow \frac{11}{2}^+$	
649.5	63	0.26±0.07	−0.18±0.09	70±4	$\frac{9}{2}^+ \rightarrow \frac{5}{2}^+$	
701.5[e]	<57	0.12±0.20			$\frac{17}{2}^+ \rightarrow \frac{13}{2}^+$	
732.0	21	0.13±0.09	−0.15±0.13		$\frac{17}{2}^+ \rightarrow \frac{13}{2}^+$	
745.9					$\frac{19}{2}^+ \rightarrow \frac{15}{2}^+$	
852.3	16	−0.80±0.20	−0.11±0.30		$\frac{13}{2}^- \rightarrow \frac{11}{2}^-$	$-0.30 < \delta < -2.2$

[a]Energies are accurate to within ±0.3 keV unless otherwise noted.

[b]I_γ, the relative intensities, have been normalized to a strong low-lying transition; typical uncertainties are ±10% except where noted.

[c]B.R. are the branching ratios of transitions from a given initial state.

[d]The $\delta(E2/M1)$ mixing ratios were extracted from the angular distribution results following Ref. 23 (paper I). An average value of the m-substate population half-width $\sigma = 2.2 \pm 0.3$, which was obtained from pure multipolarities for the (^{6}Li,3n) reaction in this region, was assumed.

[e]Doublet unresolved in the singles spectrum; evidence from coincidence data.

to hyperfine interactions,[14] the ^{116}Sn target ($\sim$10 mg/cm^2 metallic foil) was heated to $\sim$400° K. The ratio function

$$R(t) = [\mathrm{I}\,(135°,t) - \mathrm{I}\,(-135°,t)]/$$

$$[\mathrm{I}\,(135°,t) + \mathrm{I}\,(-135°,t)]\,,$$

formed from these time spectra after appropriate normalization and background subtraction, is shown in Fig. 8. The ratio data were least squares fitted with the function

$$R(t) = [3A_2/(4+A_2)]\sin 2\omega_L t\,,$$

where $\omega_L = -g\mu_N B/\hbar$ is the Larmor frequency and A_2 is the angular distribution coefficient for $P_2(\cos\theta)$. The resulting fit, shown in Fig. 8 by the solid curve, yielded a value $g = +1.21 \pm 0.08$. The small anisotropy made the measurement difficult

TABLE III. Angular distribution results for ^{121}I.

E_γ (keV)[a]	I_γ[b]	A_2	A_4	Branching ratio (B.R.) (%)[c]	$J_i \rightarrow J_f$	$\delta(E2/M1)$[d]
132.8	98	−0.13±0.06	−0.12±0.09		$\frac{7}{2}^+ \rightarrow \frac{5}{2}^+$	0.0 ±0.05
158.7	28	−0.04±0.07	−0.04±0.09		$(\frac{23}{2}^-) \rightarrow \frac{19}{2}^+$	
161.7	62	−0.14±0.06	−0.10±0.08	71±4	$\frac{11}{2}^- \rightarrow \frac{9}{2}^+$	
204.3	2			2±1	$\frac{9}{2}^+ \rightarrow \frac{7}{2}^+$	
282.4	23	−0.19±0.07	−0.12±0.10	26±4	$\frac{11}{2}^- \rightarrow \frac{9}{2}^+$	
300.9	95	0.00±0.07	−0.10±0.09	74±4	$\frac{9}{2}^+ \rightarrow \frac{7}{2}^+$	0.15±0.05
314.7	100	0.14±0.07	−0.08±0.09		$\frac{11}{2}^+ \rightarrow \frac{9}{2}^+$	0.27±0.06
328.5	54	0.11±0.07	−0.08±0.09	63±5	$\frac{13}{2}^+ \rightarrow \frac{11}{2}^+$	0.23±0.06
358.4	46	0.03±0.07	−0.12±0.09	79±3	$\frac{15}{2}^+ \rightarrow \frac{13}{2}^+$	0.18±0.05
378.6	25	0.15±0.08	−0.10±0.11	61±5	$\frac{17}{2}^+ \rightarrow \frac{15}{2}^+$	0.25±0.05
396.4	38	−0.36±0.06	−0.04±0.09	49±5	$\frac{9}{2}^+ \rightarrow \frac{7}{2}^+$	−0.20±0.05
404.4	17	0.10±0.09	−0.20±0.12	57±5	$\frac{19}{2}^+ \rightarrow \frac{17}{2}^+$	0.21±0.07
428.1	86	0.38±0.07	−0.13±0.09		$\frac{15}{2}^- \rightarrow \frac{11}{2}^-$	
433.7	34	0.15±0.07	−0.11±0.09	26±4	$\frac{9}{2}^+ \rightarrow \frac{5}{2}^+$	
445.4	34	−0.57±0.06	−0.11±0.09		$\frac{7}{2}^+ \rightarrow \frac{5}{2}^+$	−0.78±0.20
517.0	31	−0.53±0.07	−0.01±0.12	30±4	$\frac{9}{2}^+ \rightarrow \frac{7}{2}^+$	$-0.20 < \delta < -2.0$
529.4	39	0.33±0.10	−0.04±0.12	51±5	$\frac{9}{2}^+ \rightarrow \frac{5}{2}^+$	
541.2	59	0.35±0.08	−0.19±0.10		$\frac{19}{2}^- \rightarrow \frac{15}{2}^-$	
585.8	21	0.28±0.10	−0.18±0.13		$\frac{11}{2}^+ \rightarrow \frac{7}{2}^+$	
604.8	44	0.25±0.08	−0.08±0.09		$\frac{13}{2}^+ \rightarrow \frac{9}{2}^+$	
643.8	32	0.29±0.10	0.00±0.13	37±5	$\frac{13}{2}^+ \rightarrow \frac{9}{2}^+$	
645.9	33	0.35±0.11	−0.20±0.15		$\frac{23}{2}^- \rightarrow \frac{19}{2}^-$	
650.0	74	0.34±0.07	−0.16±0.09	70±4	$\frac{9}{2}^+ \rightarrow \frac{5}{2}^+$	
668.8	28	0.35±0.08	−0.17±0.11		$\frac{11}{2}^+ \rightarrow \frac{7}{2}^+$	
686.9	12	0.27±0.15	0.18±0.19	21±3	$\frac{15}{2}^+ \rightarrow \frac{11}{2}^+$	
715.4	21	0.14±0.08	−0.11±0.10		$\frac{15}{2}^+ \rightarrow \frac{11}{2}^+$	
730.2	26	0.75±0.36	−0.25±0.37		$\frac{17}{2}^+ \rightarrow \frac{13}{2}^+$	
737.0	16	0.37±0.11	−0.09±0.14	39±4	$\frac{17}{2}^+ \rightarrow \frac{13}{2}^+$	
773.5	21	0.35±0.10	−0.28±0.13		$\frac{15}{2}^+ \rightarrow \frac{11}{2}^+$	
782.9	13	0.29±0.11	−0.18±0.15	43±5	$\frac{19}{2}^+ \rightarrow \frac{15}{2}^+$	
847.3	19				$\frac{27}{2}^- \rightarrow \frac{23}{2}^-$	
864.7	20	0.48±0.10	−0.07±0.13		$\frac{21}{2}^+ \rightarrow \frac{17}{2}^+$	

[a]Energies are accurate to within ±0.3 keV unless otherwise noted.

[b]I_γ, the relative intensities, have been normalized to a strong low-lying transition; typical uncertainties are ±10% except where noted.

[c]B.R. are the branching ratios of transitions from a given initial state.

[d]The $\delta(E2/M1)$ mixing ratios were extracted from the angular distribution results following Ref. 23 (paper I). An average value of the m-substate population half-width $\sigma = 2.2 \pm 0.3$, which was obtained from pure multipolarities for the (^{6}Li,3n) reaction in this region, was assumed.

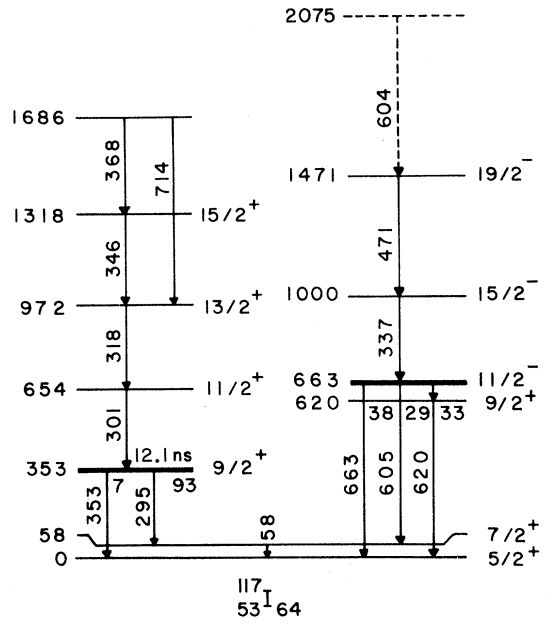

FIG. 4. Level scheme for ^{117}I extracted from the present work. All energies are in keV. The 353-keV $\frac{9}{2}^+$ level is an isomer with a half-life $t_{1/2}=12.1\pm0.7$ ns. Branching ratios given are expressed in %.

and limited the accuracy. The errors quoted include the uncertainties in the time calibration and the magnetic field. Corrections to the g factor for diamagnetism and the Knight shift are negligible compared to these uncertainties.

Because of an interest in this laboratory of a possible quadrupole moment measurement for this isomer, the g factor was measured in a different extranuclear environment via the ^{109}Ag(^{13}C,3n)^{119}I reaction by Vapirev *et al.*[15] They obtained $g=+1.20\pm0.05$ which is consistent within uncertainties but achieved an improved accuracy.

C. ^{121}I

The 301- and 434-keV deexcitation γ rays from the decay of the 434-keV $\frac{9}{2}^+$ level in ^{121}I were observed to be delayed into an early time window in the pulsed beam-γ measurements. The time differential spectra for the Compton subtracted photopeaks of both of these γ rays yielded the same lifetime result with no prompt components. The fits of these time spectra resulted in a mean lifetime $\tau=13.5\pm0.5$ ns for the 434 keV $\frac{9}{2}^+$ level in ^{121}I. This result is consistent with an independent pulsed beam-γ measurement by Hagemann *et al.*[11] via the ^{121}Sb(^{3}He,3n)^{121}I reaction which yielded $t_{1/2}=9.6\pm0.6$ ns.

A very long lived isomer, which was weakly observed at 2377 keV, fed the $\frac{19}{2}^+$ member of the $\Delta J=1$ band via a 159-keV γ ray. The lifetime of this isomer was measured by employing a ^{6}Li beam pulsed at a period of 32 μs. Integrating γ-ray intensities for the 159 keV and $\Delta J=1$ band-member transitions over four equal time windows for this time range, yielded a mean lifetime of $\tau=13\pm2$ μs. The time differential spectra for the 1 μs pulsing

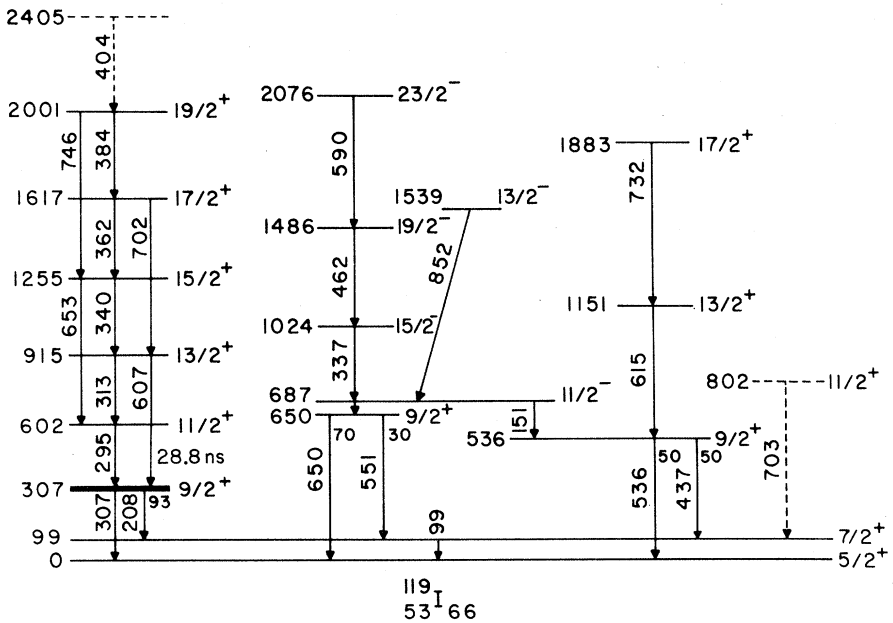

FIG. 5. Level scheme for ^{119}I extracted from the present work. All energies are in keV. The 307-keV $\frac{9}{2}^+$ level is an isomer with a half-life $t_{1/2}=28.8\pm1.0$ ns. Branching ratios given are expressed in %.

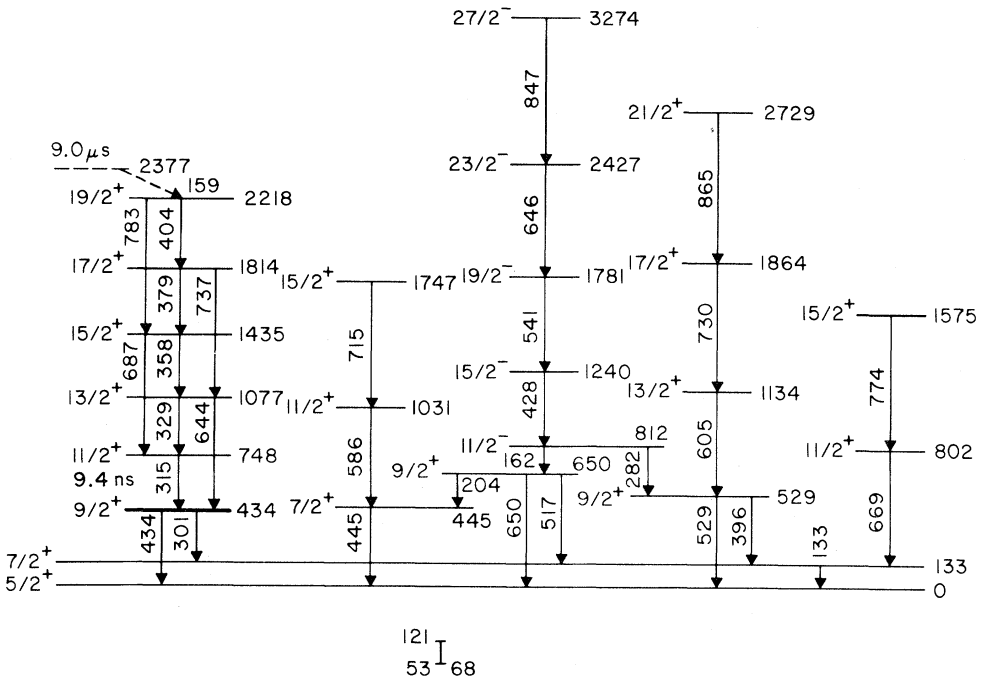

FIG. 6. Level scheme for ^{121}I extracted from the present work. All energies are in keV. The 434-keV $\frac{9}{2}^+$ level is an isomer with a half-life $t_{1/2}=9.4\pm0.4$ ns. The long lived isomer at 2377 keV has a half-life $t_{1/2}=9.0\pm1.5$ μs.

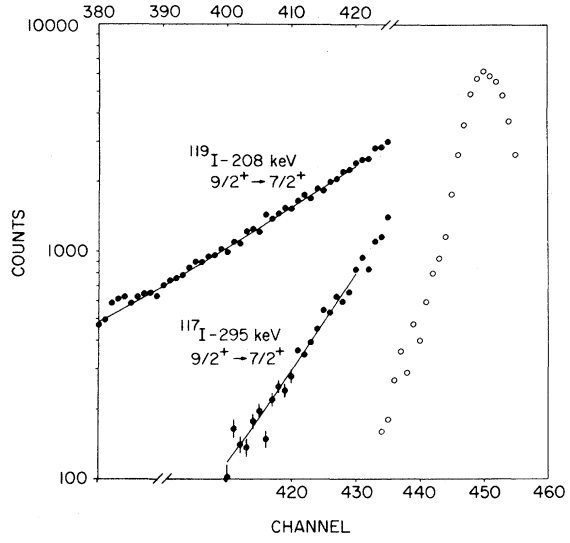

FIG. 7. Pulsed beam-γ time differential spectra for the $\frac{9}{2}^+$ isomers in ^{117,119}I. These decay curves were obtained from Compton subtracted photopeaks of the $\frac{9}{2}^+\rightarrow\frac{7}{2}^+$ transitions. The single lifetime fits to the data, represented by the solid lines, yielded half-lives of $t_{1/2}=12.1\pm0.7$ ns and 28.8 ± 1.0 ns for ^{117}I and ^{119}I, respectively. The open circles on the right show a prompt resolution function measured simultaneously for a γ ray of similar energy.

period showed that the 159-keV transition had no prompt component. This fact implies that the long lived isomer in ^{121}I is at 2377 keV.

IV. DISCUSSION

The two collective features systematically observed in the odd-mass I nuclei were (1) $\Delta J=1$

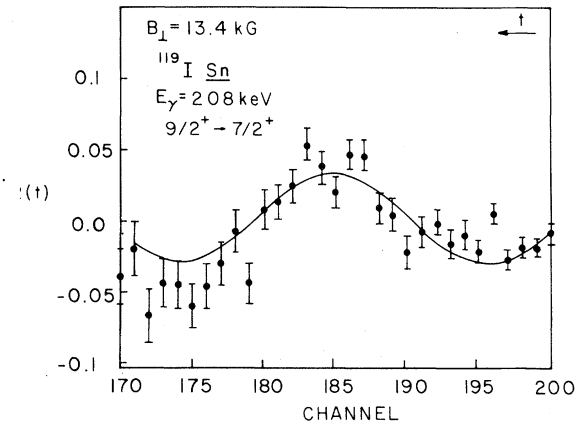

FIG. 8. The ratio function $R(t)=[I(135°,t)-I(-135°,t)]/[I(135°,t)+I(-135°,t)]$ obtained from the perturbed angular distribution measurement of the g factor for the 307-keV $\frac{9}{2}^+$ isomer in ^{119}I. The solid curve represents the $\sin2\omega_L t$ fit, which yielded $g=1.21\pm0.08$.

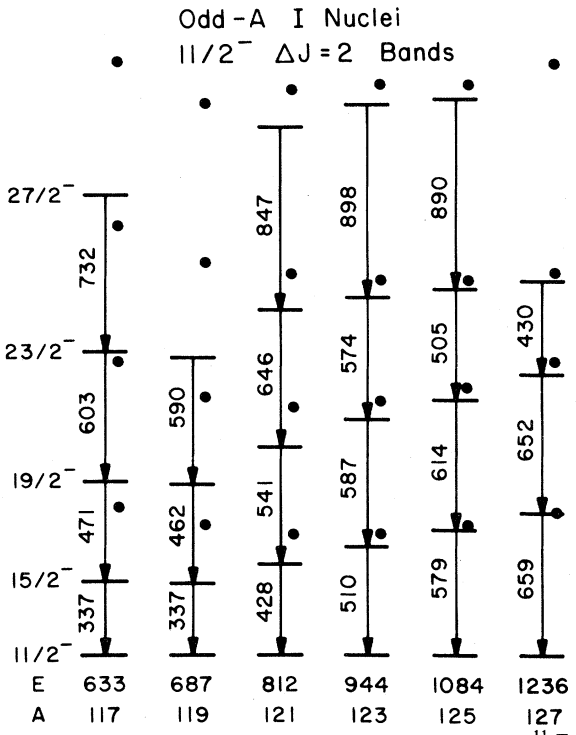

FIG. 9. Systematic $\Delta J=2$ bands built on the $\frac{11}{2}^-$ states in the odd-mass I nuclei. The filled circles represent the ground-state bands in the corresponding $^{A-1}$Te core nuclei. The γ-ray and bandhead energies are in keV.

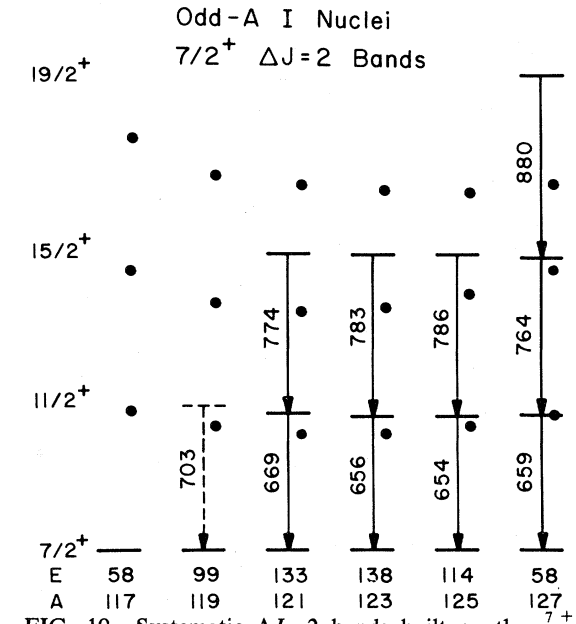

FIG. 10. Systematic $\Delta J=2$ bands built on the $\frac{7}{2}^+$ states in the odd-mass I nuclei. The filled circles represent the ground-state bands in the corresponding $^{A-1}$Te core nuclei. The γ-ray and bandhead energies are in keV.

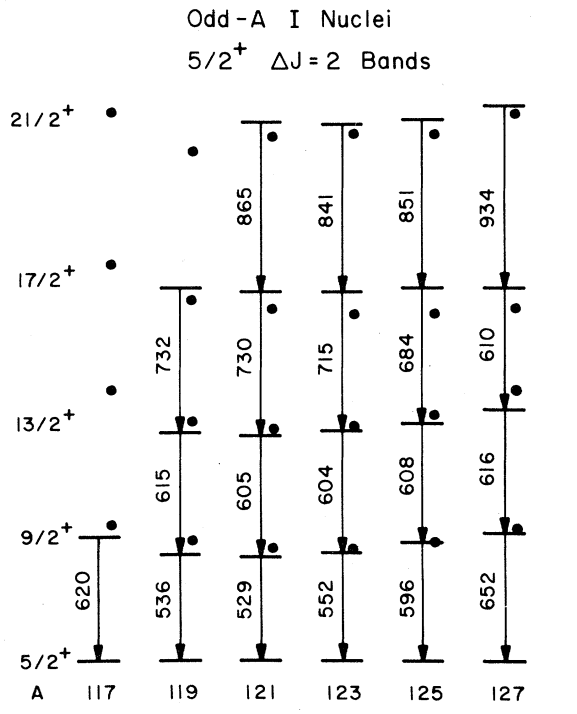

FIG. 11. Systematic $\Delta J=2$ bands built on the $\frac{5}{2}^+$ ground states in the odd-mass I nuclei. The filled circles represent the ground-state bands in the corresponding $^{A-1}$Te core nuclei.

bands built on low-lying $\frac{9}{2}^+$ states, and (2) $\Delta J=2$ bands built on $\frac{11}{2}^-$, $\frac{7}{2}^+$, and $\frac{5}{2}^+$ states. A discussion including a summary of all of the $\frac{9}{2}^+$ $\Delta J=1$ bands was given in the previous paper (I), while that for the $\Delta J=2$ bands is presented in this paper (II). The $\Delta J=2$ bands built on the $\frac{11}{2}^-$, $\frac{7}{2}^+$, and $\frac{5}{2}^+$ states, which were observed in the odd-mass I nu-

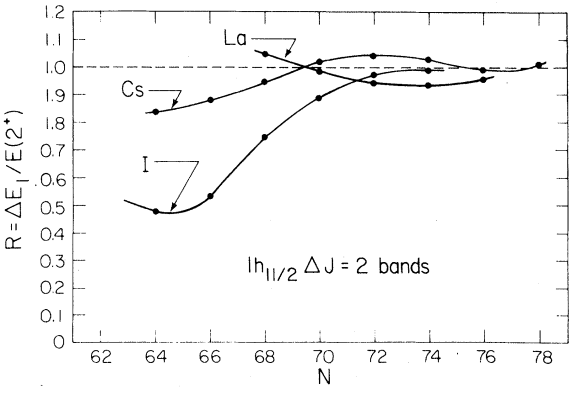

FIG. 12. Experimental R ratios of the first $\frac{11}{2}^-$ $\Delta J=2$ band spacing to the $E(2^+)$ of the $(A-1)$ core nuclei for the odd mass I, Cs (Refs. 6 and 7), and La (Refs. 3 and 8) nuclei. The curves simply connect the experimental ratios.

clei, are shown in Figs. 9–11, respectively. The filled circles, representing the ground-state band (0^+, 2^+, 4^+,...) in the corresponding $^{(A-1)}$Te core nuclei are shown in these figures for comparison purposes.

The $\Delta J=2$ bands for the odd-mass I nuclei form remarkably smooth systematic trends, which fit into the mapping of collective properties for the $Z>50$ transition region.[16] For the bands built on the $\frac{5}{2}^+$ and $\frac{7}{2}^+$ states, $\Delta J=2$ band spacings generally follow the spacings of the ground-state bands of the (Te) core nuclei shown by the filled circles; similar trends were observed[3,6–8] in the odd-mass Cs and La nuclei. A marked contrast occurs for the $\Delta J=2$ bands built on the $\frac{11}{2}^-$ states; these $\Delta J=2$ spacings, which equal the (Te) core spacings for the high-A I nuclei, decrease significantly relative to the (Te) core spacings as A decreases (see Fig. 9). This large decrease, which reaches approximately a factor of 2 for ^{117}I, was not observed for other odd-proton $\frac{11}{2}^-$ $\Delta J=2$ bands in the $Z>50$ transition region. In Fig. 12, the first $\frac{11}{2}^-$ $\Delta J=2$ band spacings ($\frac{15}{2}^- - \frac{11}{2}^-$) for the I, Cs, and La nuclei are compared with the first core spacings ($2^+ - 0^+$) for the appropriate Te, Xe, and Ba cores. As shown, the significant ratio decrease for the I nuclei takes place near the $N=64$ (^{117}I) neutron subshell closure. The Cs nuclei[6,7] show a similar but much reduced effect, while this ratio for the La nuclei[3,8] remains near 1.0. The dashed line at a ratio $R=1.0$ represents a weak coupling limit of equal spacings.

The theoretical interpretation of $\Delta J=2$ bands in transitional nuclei has usually been approached with a macroscopic particle-core coupling for either a deformed rotor[17] or an anharmonic vibrator[18] as the core. The particle states in the odd-mass I nuclei, which relate to the $\frac{11}{2}^-$, $\frac{7}{2}^+$, and $\frac{5}{2}^+$ bandheads, are consistent with the $1h_{11/2}$, $1g_{7/2}$, and $2d_{5/2}$ quasiprotons above the $Z=50$ closed proton shell. Both of these macroscopic theoretical approaches can achieve somewhat equivalent energy results for the yrast members of the $\Delta J=2$ bands.

In the particle-rotor coupling for a prolate deformed rotor, the $\Delta J=2$ bands, the so-called decoupled bands, result from the rotational alignment of the odd particle by the Coriolis interaction. Detailed calculations have been performed for the $\Delta J=2$ bands of odd-proton nuclei in the $Z>50$ transition region using both symmetric and triaxial rotors.[7,17] The deformation parameters β for the prolate rotors are varied in these calculations to fit the lower $\Delta J=2$ band spacings. The inclusion of a γ asymmetry for a triaxial rotor does not have a strong effect on the spacings, although those of higher spin are decreased somewhat out to a $\gamma\approx 25°$. Reasonable variations of the Fermi level for the odd proton as a function of N do not significantly change the results. These calculations tend to yield band spacings that are increasingly too large compared to experimental values as the spin gets larger. The introduction of a variable moment of inertia, which allows the moment of inertia of the core to increase consistent with centrifugal stretching, improves the fits at the higher spins.[17]

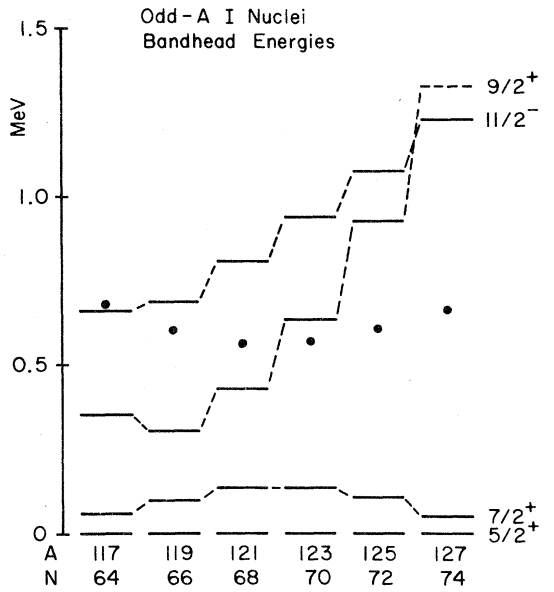

FIG. 13. Bandhead energies for the $\frac{5}{2}^+$, $\frac{7}{2}^+$, and $\frac{11}{2}^-$ $\Delta J=2$ bands and for the $\frac{9}{2}^+$ $\Delta J=1$ bands in the odd-mass I nuclei. The filled circles represent the $E(2^+)$ for the $^{A-1}$Te core nuclei.

The above calculations fit the $\Delta J=2$ decoupled bands in the odd-A nuclei and the ground-state bands of the even cores with a consistent core deformation β for those cases where the $\Delta J=2$ band spacings follow those of the core ($R\approx 1$). For the $\frac{11}{2}^-$ $\Delta J=2$ bands in the I isotopes, which have strongly reduced spacings relative to those of the Te cores ($R<1$), it has been argued[4] that the $h_{11/2}$ proton induces a larger core deformation. This would increase the moment-of-inertia of the rotor and thus reduce the $\Delta J=2$ spacings. The absence of such strong reductions in the spacings for the $\frac{5}{2}^+$ and $\frac{7}{2}^+$ $\Delta J=2$ bands in this region as well as for the $\frac{11}{2}^-$ bands in the Cs and La nuclei makes this induced deformation a complication beyond the simple particle-plus-rotor models.

The second macroscopic approach, the particle-

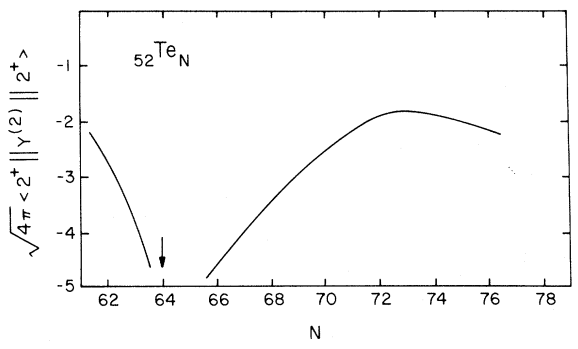

FIG. 14. The $\langle 2^+||Y^{(2)}||2^+\rangle$ core matrix elements ($^{A-1}\mathrm{Te}_N$) for the odd-mass I generalized-seniority-scheme (GSS) calculations from Ref. 19.

plus-vibrator model, likewise can achieve reasonable fits to the $\Delta J=2$ bands in these nuclei.[18] One motive for this approach comes from the fact that the smaller Coriolis interaction for the low-j particles, such as the $d_{5/2}$ and $g_{7/2}$ protons, makes it difficult to achieve the decoupling required in the rotor model for the associated $\Delta J=2$ bands. The reductions in the $\Delta J=2$ spacings relative to those of the cores are details that are not reproduced in an obvious way in this model. Although more complex, a combination of the macroscopic rotor and vibrator approaches might yield a closer approximation to the collectivity of the cores for transitional nuclei. The partial success of these macroscopic models, however, is somewhat unsatisfying due to their nonuniqueness.

To achieve a better understanding of the detailed structure of transitional nuclei, a more microscopic interpretation is desirable. Such an interpretation should include the limiting features observed for odd-A transitional nuclei in different regions, namely deformed rotor characteristics and vibrational characteristics. Recently a model that can account for a mixture of these limiting behaviors has been suggested; this model[9,19] uses the microscopic generalized seniority scheme (GSS) to describe the detailed competition between the rotational and vibrational behavior of slightly deformed nuclei. A perturbation expansion of the particle (hole)-collective core interaction has been obtained from a coherent sum of nucleon-nucleon interactions. The results include both seniority conserving (first order) terms and seniority breaking (second order) terms. Spherical nuclei have level structures characteristic of seniority conserving forces, while deformed nuclei have those of seniority breaking forces. The structure of these slightly deformed transition nuclei is governed by the competition between these two terms. The only free parameter is the nucleon-nucleon residual interaction, the strength of which is determined from ^{210}Pb. For this GSS, matrix elements of one- and two-body operators have an explicit dependence on the number of particles, which is a conserved quantity. Thus, in this model, the structure predictions for the systematic properties of odd-mass I nuclei are analytic expressions that contain a dependence on the number of neutrons N in the effective shell.

The detailed GSS calculations of the macroscopic particle (hole)-core interaction from the microscopic residual interactions give rise to diagonal core matrix elements of the $Y^{(2)}$ operator, which for the $Z>50$ transition region, do not change sign over the effective neutron shell. Thus, the transition nuclei of the $Z>50$ region are predicted to have prolate shapes throughout the entire neutron shell. The structure predictions for the odd-Z nuclei yield $\Delta J=2$ bands for the particle states and, as discussed in paper I, $\Delta J=1$ bands for the hole states. No level crossings in the band structure are expect-

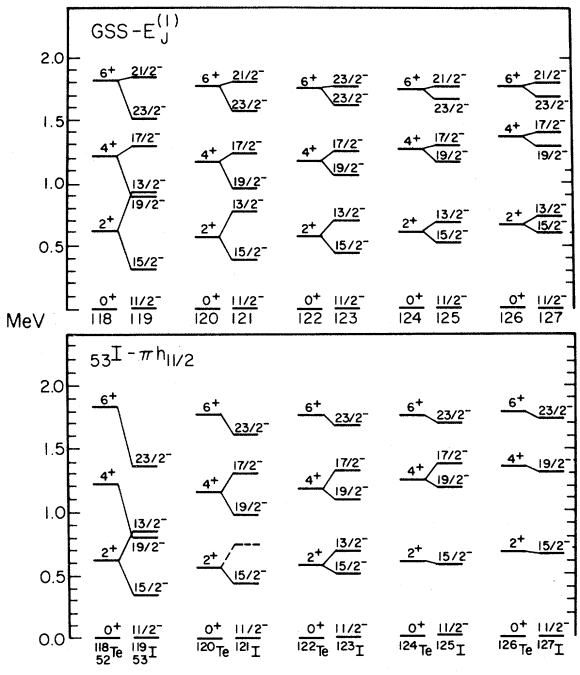

FIG. 15. The generalized-seniority-scheme (GSS) calculations of Ref. 19 for the $\Delta J=2$ bands built on the $\pi h_{11/2}$ proton states in the odd-mass I nuclei (upper part). The ground-state band of the $^{A-1}$Te core nuclei are shown to the left of each band. Experimental comparisons for the odd-mass I nuclei are shown in the bottom part (present work, Ref. 11, and Ref. 20, paper I).

ed in this transition region, because of the lack of a sign inversion for the $Y^{(2)}$ operator.

For the particle states, the seniority conserving interaction terms are dominant, yielding energies that vary linearly with N. This feature can be seen for the $h_{11/2}$ quasiproton states of the odd-mass I isotopes in Fig. 13. For the hole states, the second-order seniority breaking terms become significant. This introduces a quadratic dependence of their energies on N as shown for the $g_{9/2}$ proton-hole states in paper I. The influence of the seniority breaking terms in the odd-mass I nuclei can be seen in Fig. 13 by observing the energy differences between the $h_{11/2}$-particle states and the $g_{9/2}$-hole states. Detailed theoretical and experimental comparisons of the particle (hole) energies for the entire $Z>50$ transition region are presented in Ref. 9 for the GSS model.

The bandlike level structure of the odd-mass I nuclei is determined mainly by the first-order seniority conserving term in the GSS calculations. This term yields weak-coupling like spin multiplets, which relate to the coupling of the odd proton j_π to the core J_c. The spreading of the multiplets is determined by the $Y^{(2)}$ matrix element of the core; the N dependence[19] of the

$$\langle 2^+||Y^{(2)}||2^+\rangle$$

matrix element for the Te cores ($J_c=2$) is shown in Fig. 14. The GSS calculations[19] for the bandlike level structures of the $h_{11/2}$ proton states in the odd-mass I nuclei are presented in the upper part of Fig. 15. The $J_{\max}$ for each spin multiplet with $J_c=0, 2, 4, \ldots$ is pushed down in energy resulting in $\Delta J=2$ bands. The experimentally observed band spacings shown in the bottom part of Fig. 15 are well reproduced by the calculations. In particular, the large reduction in the odd-mass I $\Delta J=2$ band spacings compared to the Te core spacings as A decreases is explained. These calculations, in fact, are consistent with the $\pi h_{11/2}$ $\Delta J=2$ band structure for the entire $Z>50$ transition region as summarized in Fig. 12, which shows the ratio R of the $(\frac{15}{2}^- - \frac{11}{2}^-)$ spacings to the (2^+-0^+) core spacings for the I, Cs, and La isotopes as a function of A. The GSS calculations for the Cs and La nuclei give a second order term that is more important because of the smaller core spacings; this results in the ratio R remaining closer to unity. Similar calculations for the $\pi d_{5/2}$ and $\pi g_{7/2}$ particle states are more complicated because of the Pauli effect. The details of all the bandlike structure calculations for the $Z>50$ transition region will be given in Ref. 19.

The lifetime and g-factor measurements for the $\frac{9}{2}^+$ proton-hole states in ^{117,119,121}I provide additional information regarding electromagnetic properties for these transition nuclei. The measured mean lifetimes of $\tau=17.5\pm1.0$, 41.5 ± 1.5, and 9.8 ± 0.4 ns for the $\frac{9}{2}^+$ states in ^{117,119,121}I, respectively, imply hindrances of $\sim10^4$ relative to Weisskopf estimates for $M1$ transitions to the $\frac{7}{2}^+$ quasiproton states. These hindrances relate to the lack of overlap between the proton-hole and proton-particle states.

The combined g-factor results for the $\frac{9}{2}^+$ proton-hole state in ^{119}I from the present results as well as the independent measurement[15] is $g=1.20\pm0.05$. This value agrees with the GSS calculations for the $\frac{9}{2}^+$ hole states.[9] In these calculations, the proton-hole state is obtained from the coupling of the $g_{9/2}$ proton-hole to the ground state of the ^{120}Xe core, with the result that the deviation from the Schmidt limit is mainly given by the core-polarization effects.[20] The deviation from the Schmidt limit of -1.4 ± 0.2 nm for this state is consistent with the theoretical value[9] of -1.35 nm obtained from the GSS calculations. The g factors of the bandheads are not expected to be strongly dependent on the nature of the collectivity of the cores.

The $\tau=13\pm2$ μs isomer observed at 2377 keV in ^{121}I is consistent with a 159-keV $M2$ transition (Weisskopf estimate) to the $\frac{19}{2}^+$ $\Delta J=1$ band member. A stretched $M2$ transition would imply a $(\frac{23}{2}^-)$ assignment for the isomer. One possible configuration for this isomer is a negative-parity core excitation in ^{120}Te coupled to a low-lying positive parity orbital.

This work was supported in part by the National Science Foundation.

*Present address: A. W. Wright Nuclear Structure Lab., Yale University, New Haven, CT 06511.

†Present address: Brookhaven National Laboratory, Upton, NY 11973.

‡Present address: Machlett Laboratories, 1063 Hope Street, Stamford, CT 06907.

§Present address: National Bureau of Standards, FM 105, Washington, D. C. 20234.

[1] A. K. Gaigalas, R. E. Shroy, G. Schatz, and D. B. Fossan, Phys. Rev. Lett. 35, 555 (1975).

[2]R. E. Shroy, A. K. Gaigalas, G. Schatz, and D. B. Fossan, Phys. Rev. C 19, 1324 (1979).
[3]P. Chowdhury, U. Garg, A. Neskakis, W. F. Piel, Jr., T. P. Sjoreen, P. M. Stwertka, and D. B. Fossan (unpublished).
[4]D. M. Gordon, M. Gai, A. K. Gaigalas, R. E. Shroy, and D. B. Fossan Phys. Lett. 67B, 161 (1977).
[5]D. B. Fossan, M. Gai, A. K. Gaigalas, D. M. Gordon, R. E. Shroy, K. Heyde, M. Waroquier, H. Vincx, and P. Van Isacker, Phys. Rev. C 15, 1732 (1977).
[6]U. Garg, T. P. Sjoreen, and D. B. Fossan, Phys. Rev. Lett. 40, 831 (1978).
[7]U. Garg, T. P. Sjoreen, and D. B. Fossan, Phys. Rev. C 19, 207 (1979); 19, 217 (1979).
[8]F. S. Stephens, D. M. Diamond, R. M. Leigh, T. Kammuri, and K. Nakai, Phys. Rev. Lett. 29, 438 (1972).
[9]M. Gai, A. Arima, and D. Strottman, Phys. Lett. 106B, 6 (1981).
[10]*Tables of Isotopes,* 7th ed., edited by C. M. Lederer and V. S. Shirley (Wiley, New York, 1978); *Nuclear Level Schemes A=45 through A=257 from Nuclear Data Sheets,* edited by the Nuclear Data Group (Academic, New York, 1973); A. Szanto de Toledo, H. V. Klapdor, H. Hafner, W. Saathoff, E. M. Szanto, and M. Schrader, Phys. Rev. C 17, 2253 (1978).
[11]U. Hageman and H. J. Keller, in *Proceedings of the International Conference on Nuclear Structure,* Tokyo, 1977, edited by T. Marumori (Physical Society of Japan, Tokyo, 1978), p. 362.
[12]M. Blann, U. S. Atomic Energy Commission Report No. 000-3494-29.
[13]E. Recknagel, *Nuclear Spectroscopy and Reactions,* edited by J. Cerny (Academic, New York, 1974), p. 93.
[14]R. E. Shroy, G. Schatz, and D. B. Fossan, Hyp. Int. 4, 738 (1978).
[15]E. Vapirev, E. Dafni, M. H. Rafailovich, and G. D. Sprouse, Bull. Am. Phys. Soc. 23, 556 (1978).
[16]D. B. Fossan, *Structure of Medium Heavy Nuclei, Rhodes, 1979* (Institute of Physics, Bristol, 1980), pp. 151–160.
[17]F. S. Stephens, Rev. Mod. Phys. 47, 43 (1975); J. Meyer-ter-Vehn, Nucl. Phys. A249, 111 (1975); A249, 141 (1975); H. Toki and A. Faessler, *ibid.* A253, 231 (1975).
[18]U. Hagemann and F. Donau, Phys. Lett. 59B, 321 (1975); G. Alaga and V. Paar, *ibid.* 61B, 129 (1976).
[19]M. Gai, A. Arima, and D. Strottman, in *Proceedings of the International Conference on Band Structure, New Orleans, 1980,* edited by A. L. Goodman (North-Holland, Amsterdam, 1980), p. 158; and (unpublished).
[20]A. Arima and H. Horie, Prog. Theor. Phys. 12, 623 (1954).